

# Photoluminescent Ester Oligomers Containing Curcumin Dye Units: A Selective Fluorescent “Turn off” Chemosensor for Ferric Ions<sup>†</sup>

Hoay-Ching Ong and Chuan-Wei Oo\*

School of Chemical Sciences, Universiti Sains Malaysia, 11800 USM, Penang, Malaysia.

\*Corresponding author (e-mail: oocw@usm.my)

New curcumin-based ester oligomers were synthesized via polycondensation of curcumin diol with aromatic diacid. The oligomers were characterized by elemental analysis, <sup>1</sup>H-NMR, <sup>13</sup>C-NMR, FT-IR and TGA. The onset of thermal degradation was at 280°C and ester oligomers with longer alkyl chains showed lower thermal stability. Photoluminescence properties of the ester oligomers were examined by using UV-Vis and fluorescence spectroscopies. The ester oligomers exhibited green emission under UV irradiation. Selective fluorescence quenching was observed upon the addition of ferric (Fe<sup>3+</sup>) ions over other heavy metal cations. The result suggested the new curcumin-based ester oligomers can be potential chemosensors for Fe<sup>3+</sup> ions.

**Key words:** Chemosensor; oligomers; photoluminescence; thermal stability

Received: September 2019; Accepted: February 2020

Photoluminescence is a process in which electrons are excited by absorbing photon and then returned to lower energy ground state via emitting light [1]. Photoluminescence polymer sensors are being developed recently for chemical and biochemical detection as well as bioimaging by observing the fluorescence intensity changes [2]. Selectivity and sensitivity of the polymer sensors are tunable by incorporating specific functionalities such as azacrown ethers, benzothiazole, and cyclodextrin along the polymer chains either to the backbone or the side-chain [3]. Besides, fluorescein, diketopyrrolopyrrole, and terpyridine were the fluorophores that had been introduced into different conjugated polymers which enhanced the photoluminescence property of the polymers [4-6]. Curcumin is also known as fluorophore which possesses 1,3-diketone moiety that can exist in keto-enol tautomeric forms. These tautomers could act as chelating agents for metal ions [7]. Although most of the studies on curcumin-based polymers had been developed for drug carriers but there are very few curcumin-based polymer sensors [8-10].

Aromatic polyester is less processable due to its limitation in solubility. High planarity of polyester backbone limits the conformational disorder along the conjugated backbone. This enhances  $\pi$ - $\pi$  stacking interaction, and hence resulting in poor solubility [11]. In a previous study, flexible alkyl side chains were bridged by triazole ring to improve the solubility of material owing to the rigid structure of conjugated backbones [12]. In addition, the triazole ring had been proven to enhance the thermal stability of the studied material and it showed excellent cations binding motifs [13,14].

The objectives of this study were to synthesize and characterize new conjugated ester oligomers containing curcumin in the backbone with enhanced solubility by incorporating alkyl groups with different lengths in the side-chains. The thermal behavior of the synthesized ester oligomers and their potential as chemosensors toward heavy metal ions were investigated.

## EXPERIMENTAL

### Materials

Curcumin, 5-hydroxyisophthalic acid, 1-bromodecane, 1-bromododecane, 1-bromotetradecane, copper(II) sulfate pentahydrate, thionyl chloride, and sodium azide were purchased from Merck (Darmstadt, Germany). Potassium hydroxide and potassium iodide were purchased from Q-rec Chemicals (New Zealand). Propargyl bromide and 1-bromohexadecane were purchased from Tokyo Chemical Industry (Tokyo, Japan). Potassium carbonate and sodium ascorbate were obtained from Sigma-Aldrich (St. Louis, MO, USA). Triethylamine was obtained from R&M Chemicals (Alberta, Canada). All the chemicals were used as received without further purification.

### Physicochemical Characterization

The synthesized monomers and ester oligomers were analyzed by Perkin Elmer ATR-FTIR at the frequency range of 4000-500 cm<sup>-1</sup>. Bruker Avance 500 MHz ultrashield spectrometer equipped with ultrashield magnets was used to record the <sup>1</sup>H and <sup>13</sup>C-NMR spectra of the monomers and ester oligomers. Mettler 851e thermogravimetric analyser was used for TGA

<sup>†</sup>Paper presented at the 7th International Conference for Young Chemists (ICYC 2019), 14-16 August 2019, Universiti Sains Malaysia.

analysis on the synthesized ester oligomers in nitrogen atmosphere with the heating rate of  $10^{\circ}\text{C min}^{-1}$ . The number of averaged molecular weight, weight-molecular weight and dispersity index were obtained via gel permeation chromatography (GPC) equipped with Waters 1515 isocratic HPLC pump and Waters 2414 refractive index detector. The calibration was done using polystyrene as the standard and GPC grade THF was used as the eluent. UV-Vis and fluorescence spectra were recorded on Shimadzu UV-2600 UV-Vis spectrophotometer and LS-55 fluorescence spectrophotometer, respectively, with quartz cell (1 cm  $\times$  1 cm).

### Synthesis of Monomers and Ester Oligomers

All the monomers and ester oligomers were synthesized according to the synthesis route as shown in Scheme 1. 5-Hydroxyisophthalic acid (6.00 g, 32.91 mmol) was refluxed in 12 mL absolute ethanol with a catalytic amount of  $\text{H}_2\text{SO}_4$  for 8 h. The resultant mixture was extracted with diethyl ether to yield **S1**. Then, propargyl bromide (2.55 g, 21.41 mmol) was mixed with **S1** (4.00 g, 17.84 mmol) in acetone. 2 molar equivalent of potassium carbonate and a catalytic amount of potassium iodide were added into the mixture. The reaction mixture was refluxed for 12 h and the precipitate formed was recrystallized using ethanol to yield **S3**. Sodium azide (1.95 g, 30 mmol) was added into  $\text{N,N}'$ -dimethylformamide solution containing the corresponding 1-bromoalkane (15 mmol), then refluxed for 8 h. The resultant mixture was filtered, and the filtrate was extracted with dichloromethane. **S2**, a yellow oily liquid was obtained after evaporation. **S3** was added into  $\text{N,N}'$ -dimethylformamide solution containing equimolar of the corresponding **S2** (15 mmol), 20 mol % of  $\text{CuSO}_4 \cdot 5\text{H}_2\text{O}$  and 20 mol % sodium ascorbate. The reaction mixture was left stirred at ambient temperature for 24 h. The obtained precipitate after pouring into cold water was recrystallized from ethanol to yield **S4**. **S4** was subsequently refluxed with 2 molar equivalent of potassium hydroxide in ethanol for 5 h. The resulted mixture was neutralized to yield the corresponding monomers.

#### MS10-MS16.

Monomer (**MS10**): 81% yield. ATR-FTIR ( $\text{cm}^{-1}$ ): 3081, 3167-2549, 2915, 2847, 1695, 1595 and 1280.  $^1\text{H-NMR}$  ( $\text{DMSO-d}_6$ )  $\delta/\text{ppm}$ : 8.21 (1H, s, H2), 8.09 (1H, t,  $J=1.8, 1.3$  Hz, H4), 7.75 (2H, d,  $J=1.4$  Hz, H1/H1'), 5.28 (2H, s, H3), 4.34-4.37 (2H, t,  $J=7.0$  Hz, H5), 1.77-1.82 (2H, quint,  $J=7.1$  Hz, H6), 1.15-1.27 (14H, m, H7-H13), 0.83-0.86 (3H, t,  $J=6.9$  Hz, H14).  $^{13}\text{C-NMR}$  ( $\text{DMSO-d}_6$ )  $\delta/\text{ppm}$ : 166.8, 158.6, 142.7, 133.1, 124.9, 123.0, 120.0, 62.3, 49.9, 31.7-26.2, 22.5, 14.4.

Monomer (**MS12**): 84% yield. ATR-FTIR ( $\text{cm}^{-1}$ ): 3084, 3211-2571, 2912, 2853, 1698, 1594 and 1273.  $^1\text{H-NMR}$  ( $\text{DMSO-d}_6$ )  $\delta/\text{ppm}$ : 8.21 (1H, s, H2), 8.09 (1H, t,  $J=1.8, 1.3$  Hz, H4), 7.75 (2H, d,  $J=1.4$  Hz,

H1/H1'), 5.28 (2H, s, H3), 4.33-4.36 (2H, t,  $J=7.0$  Hz, H5), 1.76-1.82 (2H, quint,  $J=7.1$  Hz, H6), 1.20-1.25 (18H, m, H7-H15), 0.84-0.86 (3H, t,  $J=6.9$  Hz, H16).  $^{13}\text{C-NMR}$  ( $\text{DMSO-d}_6$ )  $\delta/\text{ppm}$ : 166.8, 158.6, 142.7, 133.1, 124.9, 123.1, 120.0, 62.2, 49.9, 31.7-26.1, 22.5, 14.3.

Monomer (**MS14**): 82% yield. ATR-FTIR ( $\text{cm}^{-1}$ ): 3099, 3371-2579, 2912, 2846, 1699, 1594 and 1273.  $^1\text{H-NMR}$  ( $\text{DMSO-d}_6$ )  $\delta/\text{ppm}$ : 8.21 (1H, s, H2), 8.09 (1H, t,  $J=1.8, 1.3$  Hz, H4), 7.75 (2H, d,  $J=1.4$  Hz, H1/H1'), 5.28 (2H, s, H3), 4.33-4.36 (2H, t,  $J=7.0$  Hz, H5), 1.77-1.80 (2H, quint,  $J=7.1$  Hz, H6), 1.21-1.25 (22H, m, H7-H17), 0.83-0.85 (3H, t,  $J=6.9$  Hz, H18).  $^{13}\text{C-NMR}$  ( $\text{DMSO-d}_6$ )  $\delta/\text{ppm}$ : 166.8, 158.6, 142.7, 133.1, 124.9, 123.1, 120.0, 62.2, 49.9, 31.8-26.2, 22.5, 14.3.

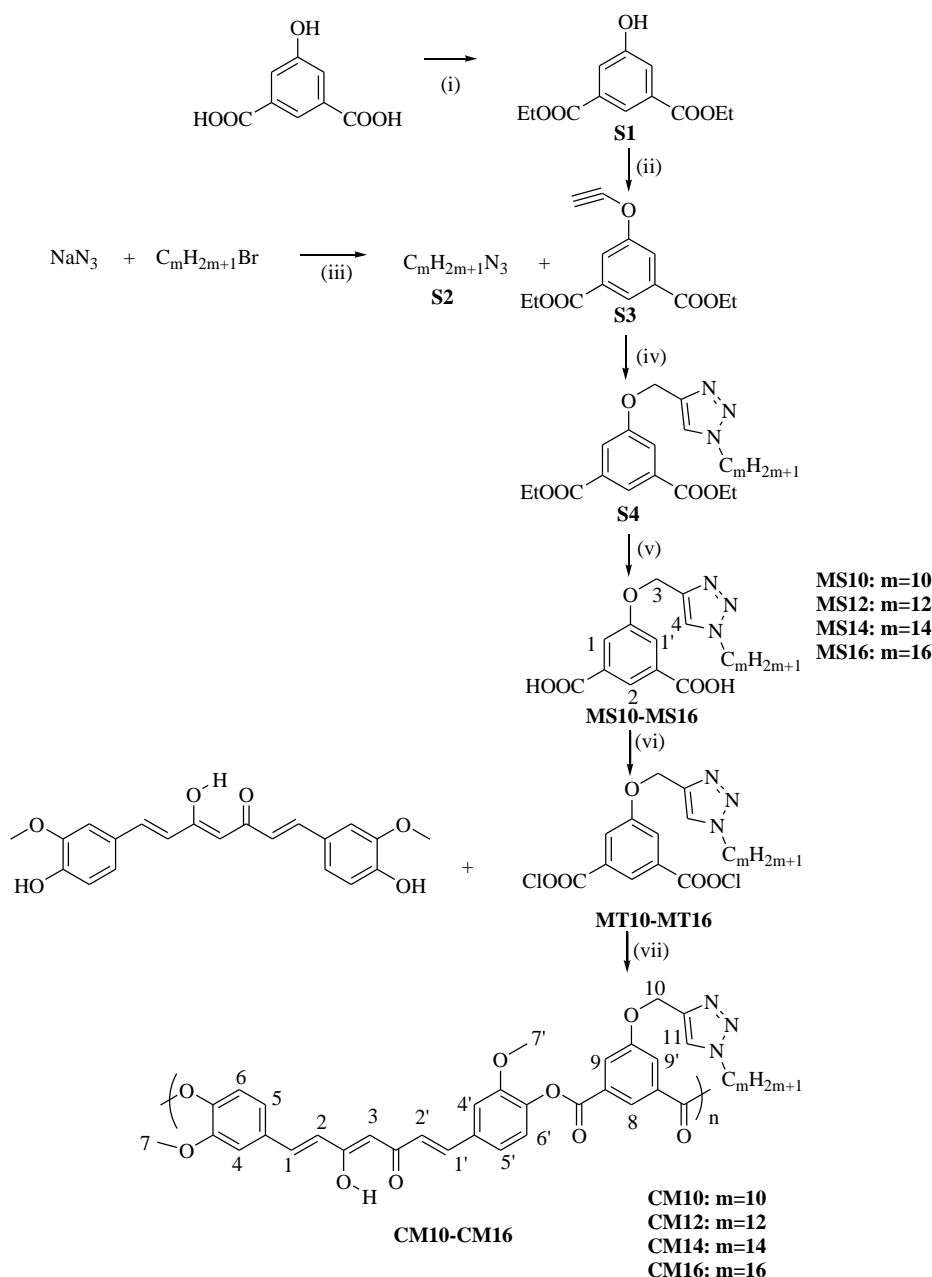
Monomer (**MS16**): 81% yield. ATR-FTIR ( $\text{cm}^{-1}$ ): 3099, 3371-2579, 2912, 2846, 1695, 1594 and 1270.  $^1\text{H-NMR}$  ( $\text{DMSO-d}_6$ )  $\delta/\text{ppm}$ : 8.21 (1H, s, H2), 8.09 (1H, t,  $J=1.8, 1.3$  Hz, H4), 7.75 (2H, d,  $J=1.4$  Hz, H1/H1'), 5.27 (2H, s, H3), 4.33-4.36 (2H, t,  $J=7.0$  Hz, H5), 1.76-1.81 (2H, quint,  $J=7.1$  Hz, H6), 1.27-1.18 (26H, m, H7-H19), 0.83-0.85 (3H, t,  $J=6.9$  Hz, H20).  $^{13}\text{C-NMR}$  ( $\text{DMSO-d}_6$ )  $\delta/\text{ppm}$ : 166.8, 158.6, 142.7, 133.1, 124.9, 123.1, 120.0, 62.2, 49.9, 31.7-26.2, 22.5, 14.4.

The ester oligomers were synthesized using the acylated monomers. **MS10-MS16** were refluxed with thionyl chloride and a catalytic amount of  $\text{N,N}'$ -dimethylformamide in benzene for 3 h to yield **MT10-MT16**, which were then directly mixed with THF/triethylamine. The resultant mixture was stirred overnight and poured into methanol to form the desired ester oligomers, **CM10-CM16**.

Oligomer (**CM10**): 49% yield. ATR-FTIR ( $\text{cm}^{-1}$ ): 3344-3555, 3084, 2925, 2853, 1742, 1627, 1593, 1192 and 1162.  $^1\text{H-NMR}$  ( $\text{CDCl}_3$ )  $\delta/\text{ppm}$ : 15.96 (OH, s, br), 8.66 (1H, s, H8), 8.08 (2H, s, H9/H9'), 7.63-7.71 (5H, m, H1/H1', H5/H5', H11), 7.29-7.17 (4H, s, H4/H4', H6/H6'), 6.59, (2H, d, H2/H2'), 5.89 (1H, s, H3), 5.36 (2H, s, H10), 4.39 (2H, s, H12), 3.88 (6H, s, H7/H7'), 1.93 (2H, s, H13), 1.26-1.40 (14H, m, H14-H20), 0.88 (3H, t, H21).  $^{13}\text{C-NMR}$  ( $\text{CDCl}_3$ )  $\delta/\text{ppm}$ : 183.1, 163.4, 158.6, 151.5, 142.9, 141.3, 139.9, 134.3, 131.2, 129.3, 124.5, 123.3, 122.9, 122.12, 121.1, 111.7, 101.9, 62.5, 56.0, 50.7, 31.8, 26.5-31.8, 22.6, 14.1.

Oligomer (**CM12**): 48% yield. ATR-FTIR ( $\text{cm}^{-1}$ ): 3621-3251, 3081, 2924, 2854, 1742, 1627, 1594, 1189 and 1156.  $^1\text{H-NMR}$  ( $\text{CDCl}_3$ )  $\delta/\text{ppm}$ : 15.96 (OH, s, br), 8.66 (1H, s, H8), 8.07 (2H, s, H9/H9'), 7.65-7.70 (5H, m, H1/H1', H5/H5', H11), 7.28-7.19 (4H, s, H4/H4', H6/H6'), 6.59, (2H, d, H2/H2'), 5.90 (1H, s, H3), 5.34 (2H, s, H10), 4.38 (2H, s, H12), 3.89 (6H, s, H7/H7'), 1.93 (2H, s, H13), 1.26-1.34 (18H, m, H14-H22), 0.88 (3H, t, H23).  $^{13}\text{C-NMR}$  ( $\text{CDCl}_3$ )  $\delta/\text{ppm}$ : 183.1, 163.4, 158.6, 151.5, 142.9, 141.3, 139.9, 134.3, 131.2, 129.3, 124.5, 123.3, 122.9, 122.1, 121.1, 111.7, 101.9, 62.5, 56.0, 50.7, 31.8, 26.5-31.8, 22.6, 14.1.

**Scheme 1.** Reagents and reaction conditions: (i)  $\text{H}_2\text{SO}_{4,\text{conc}}$  (dropwise), reflux, ethanol, 24 h.; (ii) propargyl bromide (1.2 equiv.),  $\text{K}_2\text{CO}_3$  (2 equiv.), reflux, acetone, 12 h.; (iii) sodium azide (2 equiv.), DMF,  $80^\circ\text{C}$ , 8 h.; (iv) 20 mol% of sodium ascorbate, 20 mol% of  $\text{CuSO}_4 \cdot 5\text{H}_2\text{O}$ , DMF, r. t., 24 h.; (v)  $\text{KOH}$  (2 equiv.), reflux, ethanol, 7 h.; (vi)  $\text{SOCl}_2$  (8 equiv.), DMF (dropwise), reflux, benzene.; (vii) triethylamine (2 equiv.), THF, r.t., overnight.



Oligomer (**CM14**): 51% yield. ATR-FTIR ( $\text{cm}^{-1}$ ): 3622-3292, 3080, 2924, 2853, 1742, 1628, 1593, 1190 and 1160.  $^1\text{H-NMR}$  ( $\text{CDCl}_3$ )  $\delta$ /ppm: 15.87 (OH, s, br), 8.59 (1H, s, H8), 8.00 (2H, s, H9/H9'), 7.61-7.52 (5H, m, H1/H1', H5/H5', H11), 7.19-7.10 (4H, s, H4/H4', H6/H6'), 6.51, (2H, d, H2/H2'), 5.79 (1H, s, H3), 5.29 (2H, s, H10), 4.30 (2H, s, H12), 3.80 (6H, s, H7/H7'), 1.85 (2H, s, H13), 1.17-1.20 (22H, m, H14-H24), 0.80 (3H, t, H25).  $^{13}\text{C-NMR}$  ( $\text{CDCl}_3$ )  $\delta$ /ppm: 183.1, 163.4, 158.6, 151.5, 142.8, 141.2, 139.9, 134.3, 131.2, 129.3, 124.4, 123.3, 122.9, 122.2, 121.1, 111.7, 102.0, 62.5, 56.0, 50.7, 31.9, 26.5-30.3, 22.7, 14.1.

Oligomer (**CM16**): 51% yield. ATR-FTIR ( $\text{cm}^{-1}$ ): 3680-3266, 3088, 2923, 2853, 1742, 1629, 1594, 1190 and 1159.  $^1\text{H-NMR}$  ( $\text{CDCl}_3$ )  $\delta$ /ppm: 15.96 (OH, s, br), 8.59 (1H, s, H8), 8.00 (2H, s, H9/H9'), 7.60-7.52 (5H, m, H1/H1', H5/H5', H11), 7.19-7.10 (4H, s, H4/H4', H6/H6'), 6.52, (2H, d, H2/H2'), 5.80 (1H, s, H3), 5.28 (2H, s, H10), 4.30 (2H, s, H12), 3.80 (6H, s, H7/H7'), 1.85 (2H, s, H13), 1.17-1.26 (26H, m, H14-H26), 0.80 (3H, t, H27).  $^{13}\text{C-NMR}$  ( $\text{CDCl}_3$ )  $\delta$ /ppm: 183.1, 163.4, 158.6, 151.5, 143.0, 141.3, 139.9, 134.3, 131.2, 129.3, 124.5, 123.3, 122.8, 122.2, 121.1, 111.7, 101.9, 62.6, 56.0, 50.6, 31.9, 26.5-30.3, 22.7, 14.1.

### UV-Vis Absorption and Photoluminescence Measurements

Series of **CM10-CM16** solutions with the concentration of  $8.0 \times 10^{-4}$  mg mL<sup>-1</sup> were prepared in THF solution. 30  $\mu$ M of Cu<sup>2+</sup>, Ni<sup>2+</sup>, Fe<sup>3+</sup>, Cd<sup>2+</sup>, Zn<sup>2+</sup>, and Pb<sup>2+</sup> solutions were prepared using deionized water. Metal sensing tests were carried out by titrating 30  $\mu$ M of metal ions into 3 mL of **CM10-CM16** in the 1 cm quartz cell. **CM10** was titrated with different concentrations of Fe<sup>3+</sup> solution in the range of 0-30  $\mu$ M for sensitivity test. The UV-Vis absorption and photoluminescence spectra for these solutions were recorded.

### RESULTS AND DISCUSSION

Structures of the synthesized ester oligomers were elucidated using FT-IR, <sup>1</sup>H-NMR, and <sup>13</sup>C-NMR spectroscopies. Since all the synthesized ester oligomers, **CM10-CM16** exhibited similar characteristics in their FT-IR, <sup>1</sup>H-NMR, and <sup>13</sup>C-NMR spectra, homologous **CM10** was selected for further discussion. The presence of C=O ester gave rise to an absorption band at 1742 cm<sup>-1</sup> which confirmed the completeness of esterification reaction that formed the desired ester oligomers [15]. The presence of ester functionality was further substantiated by the appearance of strong absorption band at 1192 cm<sup>-1</sup> which could be ascribed to the stretching of C-O-C ester [16]. <sup>1</sup>H-NMR of **CM10** illustrated broad signals with increased complexity which suggested the occurrence of polymerization [17]. A broad signal which resonated at  $\delta = 15.96$  ppm could be assigned to hydroxyl proton on the oxygen atom in the enol. Carbon signals at  $\delta = 183.11$  and 101.93 ppm could be attributed to the carbonyl carbon of curcumin and methine carbon attached to H3, respectively. These indicated the presence of keto-enol tautomer of curcumin moiety in **CM10** [18].

The GPC results showed the number-average

molecular weight (Mn) and weight average molecular weight (Mw) which were found to be in the range of 1284-2294 gmol<sup>-1</sup> and 1971-6239 gmol<sup>-1</sup>, respectively. Polydispersity index (PDI) was obtained in the range of 1.78-2.72. Degree of polymerization of **CM10**, **CM12**, **CM14**, and **CM16** were 3, 8, 2, and 3, respectively.

**CM10-CM16** were found to be insoluble in polar protic solvents such as water, methanol, and ethanol, as well as n-hexane and benzene which are non-polar solvents. However, the synthesized ester oligomers were soluble in common polar aprotic solvents such as chloroform, tetrahydrofuran and dichloromethane, and partially soluble in acetone as well as N,N'-dimethylformamide due to the tetrahedral nature of the alkyl chains arranged at different planes compared to the conjugated backbone. As such, these alkyl chains prevented molecular chain packing to a certain extent and increased the solubility of the oligomers [12]. The unreported curcumin-based ester oligomer with a shorter alkyl chain of two carbon atoms was found to be partially soluble even in hot organic solvents. The longer alkyl chains increased the steric hindrance and caused the ester oligomer chains to become less packed, hence, increased the free volume of the ester oligomers. This improved the diffusion of solvent molecules within the oligomer network causing it to swell and eventually dissolve.

### Thermal Properties of CM10-CM16

The thermal properties of ester oligomers **CM10-CM16** were examined via thermogravimetric analysis under nitrogen atmosphere with the heating rate of 10°C min<sup>-1</sup> from 30°C to 700°C. The onset thermal degradation temperature of the ester oligomers was recorded at 280°C. The temperature for 50% weight loss (T<sub>d50%</sub>) of **CM10-CM16** and their percentage char yield decreased with the increase in the length of the alkyl chains (m=10 to 16).

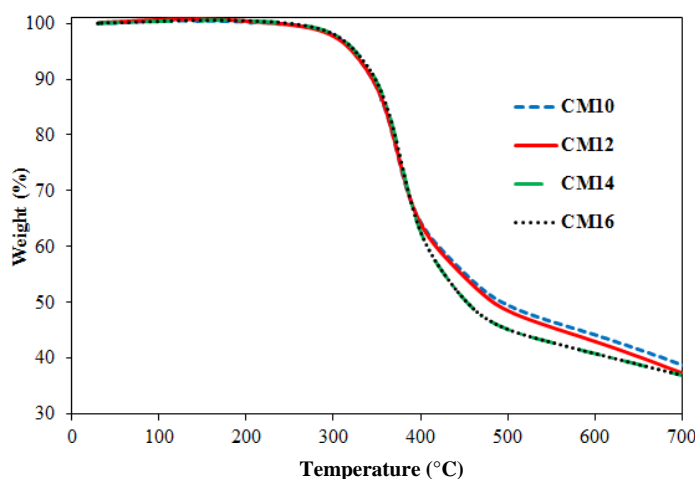


Figure 1. TGA thermograms of **CM10-CM16**

**Table 1.** Thermal decomposition values of **CM10-CM16**

Ester oligomer	T <sub>d50%</sub> (°C)	Char yield at 700°C (%)
<b>CM10</b>	494	39
<b>CM12</b>	483	37
<b>CM14</b>	458	36
<b>CM16</b>	453	32

T<sub>d50%</sub> for **CM10-CM16** were recorded at 494, 483, 458, and 453°C, respectively. The percentage of char yield at 700°C for the ester oligomers were 39%, 37%, 36%, and 32 %, respectively. Hence, the thermal stability of the ester oligomers was found to be affected by the length of the alkyl chains. The longer the alkyl chains, the lower the thermal stability of the ester oligomers. This could be attributed to the increase of steric hindrance upon increasing the length of alkyl chains which disrupted the packing of the oligomer chains, and thus reduced the intermolecular interaction. However, the shorter alkyl chain led to less steric hindrance and lower flexibility to the oligomer chain. This created a more rigid oligomer network as oligomer packing became denser which enhanced the intermolecular interaction with higher thermal stability [19]. Data from the thermogravimetric analysis of **CM10-CM16** are illustrated in Table 1.

#### Selectivity of **CM10-CM16** on Metal Ions

The response of the ester oligomers towards different metal ions namely Zn<sup>2+</sup>, Ni<sup>2+</sup>, Fe<sup>3+</sup>, Cd<sup>2+</sup>, Cu<sup>2+</sup>, and Pb<sup>2+</sup> was investigated and changes on their fluorescence intensity were recorded using UV-Vis and fluorescence spectrophotometers. Since the spectra for all the homologous oligomers showed similar characteristics, only **CM10** is discussed in detail. As shown in Figure 2a, λ<sub>max</sub> of free **CM10** recorded at 403 nm was assigned to π→π\* for the enol structure of curcumin moiety, whereas absorption at 284 nm was due to π→π\* for the keto structure [20]. When **CM10** was excited at 403 nm, green emission

was recorded with emission maxima at 505 nm (Figure 2b).

As **CM10-CM16** showed similar metal sensing abilities which were not affected by the length of the alkyl chains, therefore, only **CM10** is discussed in detail. UV-Vis absorption of **CM10** showed significant changes upon addition of Fe<sup>3+</sup> compared to other metal ions in which λ<sub>max</sub> at 403 nm was blue shifted to 370 nm with decreased molar absorptivity. A new low intense absorption band was recorded in the range of λ= 418 to 650 nm (Figure 3a). All metal ions reduced the fluorescence intensity of **CM10**, especially Fe<sup>3+</sup> by 3.1-fold as shown in Figure 3b.

Selectivity of **CM10** was further investigated by adding various metal ions to **CM10** in the presence of Fe<sup>3+</sup> (red bar). I<sub>0</sub>/I was the relative fluorescence intensity in which I<sub>0</sub> and I represented initial and final fluorescence intensity, respectively. Hence, the more the quenching, the higher the value of I<sub>0</sub>/I. The values of relative fluorescence intensity, I<sub>0</sub>/I as indicated by red bars were almost similar with the bar caused by Fe<sup>3+</sup> alone (Figure 4). This observation illustrated that detection of Fe<sup>3+</sup> was not interfered by other 30 μM equivalent competitive metal ions [21]. The responsible quencher is unlikely to be differentiated when lower concentration of Fe<sup>3+</sup> (<10 μM) and higher concentration of other metal ions coexisted. However, the presence of Fe<sup>3+</sup> could be identified via UV-Vis spectroscopy as only Fe<sup>3+</sup> will cause the blue shifting at λ= 403 nm and with increased absorption band in the range of λ= 418 to 650 nm (Figure 3a).

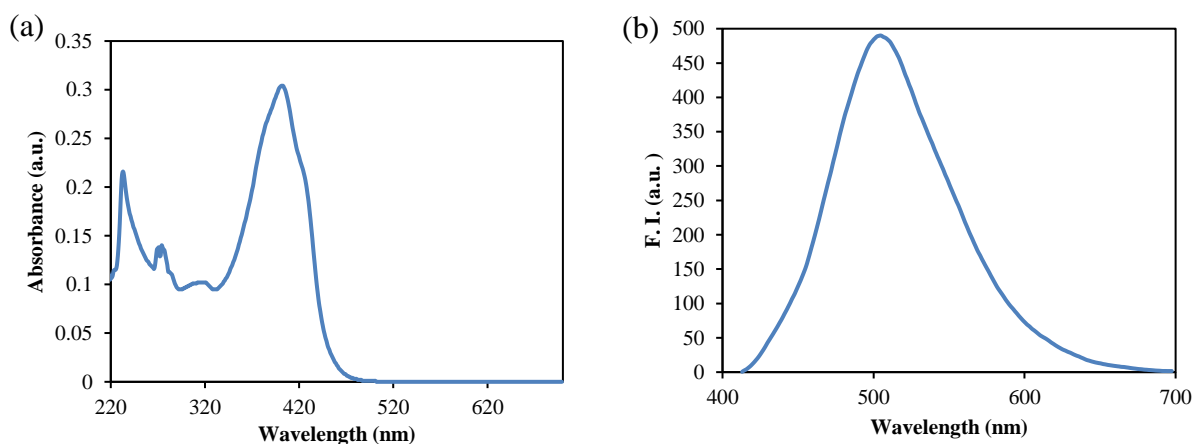


**Figure 2.** (a) UV-Vis spectrum; (b) Fluorescence spectrum of  $8.0 \times 10^{-4}$  mg mL<sup>-1</sup> **CM10** in tetrahydrofuran with λ<sub>ex</sub>= 403 nm

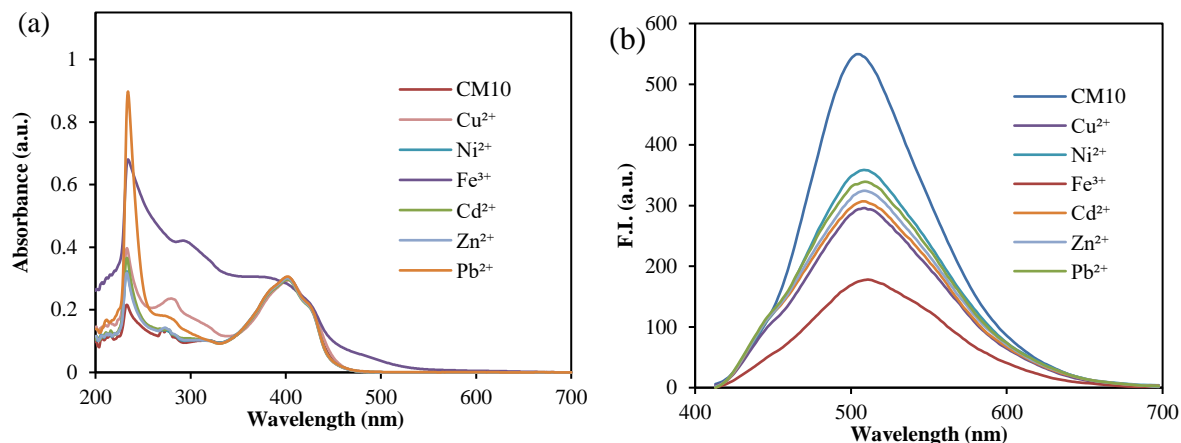


**Figure 3.** (a) UV-Vis spectra; (b) Fluorescence spectra of **CM10** in tetrahydrofuran after addition of various metal ions (30  $\mu\text{M}$ )

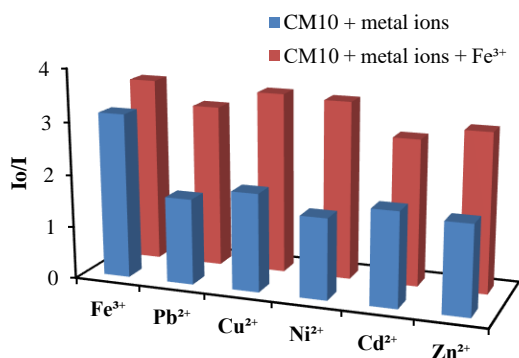


**Figure 4.** Relative fluorescence intensity of **CM10** with various metal ions at 30  $\mu\text{M}$  (blue bar) and with the presence of additional 30  $\mu\text{M}$  of Fe<sup>3+</sup> (red bar). The emission wavelength observed was 505 nm.

Besides, two isosbestic points at  $\lambda=369, 433$  nm were recorded based on the UV-Vis spectra obtained with different concentrations of Fe<sup>3+</sup> (Figure 5a). The presence of isosbestic points indicated the formation of a new ground-state species which was in equilibrium with the free **CM10** [22]. The formation of this nonfluorescent new ground-state species was responsible to the observed fluorescence quenching

effect because the nonfluorescent fluorophore-quencher species absorbed light and immediately returned to the ground state without emission of photon. The fluorescence intensity of **CM10** decreased gradually with increasing Fe<sup>3+</sup> concentration without any significant spectral shape changes (Figure 5b) which suggested the negligible formation of excited charge-transfer complex (exciplex) that happened during the excited state lifetime [23].

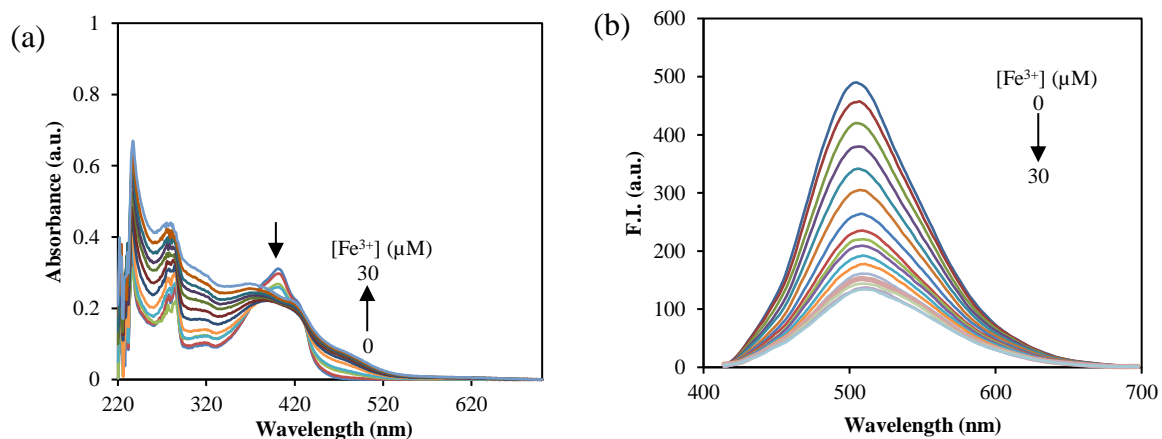


**Figure 5.** (a) UV-Vis absorbance; (b) Photoluminescence of **CM10** with various concentration of Fe<sup>3+</sup>

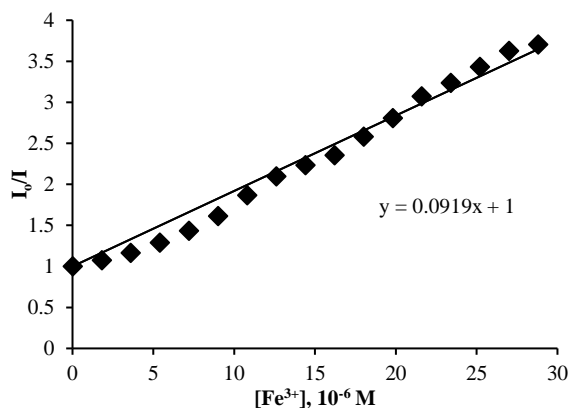


**Figure 6.** Stern-Volmer plot for the quenching fluorescence of **CM10** by  $\text{Fe}^{3+}$

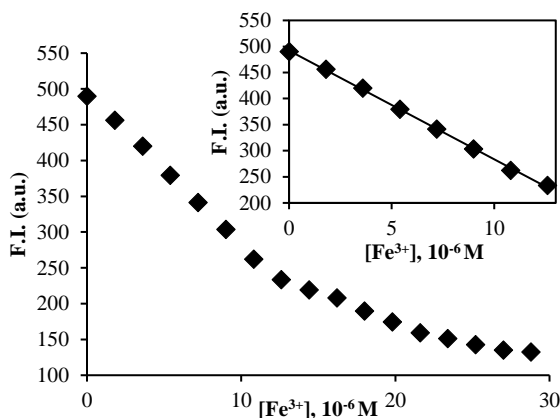


**Figure 7.** **CM10** versus increasing concentration of  $\text{Fe}^{3+}$ ; inset shows the plot of linear range of fluorescence intensity **CM10** versus concentration of  $\text{Fe}^{3+}$

**Table 2.** Limit of detection of **CM10** and other reported chemosensors towards  $\text{Fe}^{3+}$

Chemosensor	Limit of detection, $\mu\text{M}$	Reference
Quinoline derivatives	0.12	[27]
Poly(fluorine) derivatives	0.22	[27]
Propane-1,3-dione based polymer	0.4	[27]
Rhodamine derivatives	0.4	[27]
Anthracene Schiff base derivatives	0.59	[28]
Spirosazine derivatives	0.88	[27]
Benzimidazole derivatives	1.21	[27]
Julolidinie derivatives	6.8	[27]
<b>CM10</b> ester oligomers	7.90	Present work
Coumarin based polymer	10.6	[30]
Diethylenetriamine Schiff base derivative	60.49	[31]

A linear Stern-Volmer relationship between **CM10** and  $\text{Fe}^{3+}$  was obtained as shown in Figure 6, in which  $I_0$  and  $I$  represented initial and final fluorescence intensity, respectively. This indicated the dominance of fluorescence quenching process by the formation of a new ground-state species, which was proved by UV-Vis experiment (Figure 5a). According

to equation:  $I_0/I = K_{\text{SV}}[\text{Fe}^{3+}] + 1$ , the Stern-Volmer quenching constant,  $K_{\text{SV}}$  was  $9.19 \times 10^3 \text{ M}^{-1}$  [24].

The linear detection range for  $\text{Fe}^{3+}$  determination was from 0 to  $12.6 \times 10^{-6} \text{ M}$  by plotting the fluorescence intensity against concentration of  $\text{Fe}^{3+}$  as shown in Figure 7. Linear equation thus

obtained,  $I_0/I = -20.841[\text{Fe}^{3+}] + 492.05$ ,  $R^2 = 0.999$ . The detection limit was calculated by using the equation:  $\text{detection limit} = 3S/\rho$ , where  $S$  is the standard deviation of blank measurement and  $\rho$  is the slope of fluorescence intensity plotted against analyte concentration [25]. The calculated detection limit for  $\text{Fe}^{3+}$  (7.90  $\mu\text{M}$ ) was lower than the maximum limit of  $\text{Fe}^{3+}$  that is allowed by the Malaysian standards for water quality (EQA, 1974) (18  $\mu\text{M}$ ) and WHO for drinking water quality (WHO, 1993) (18  $\mu\text{M}$ ), and the irrigation water quality standards (Fipps, 2003) (90  $\mu\text{M}$ ) [26]. Table 2 shows the comparison between the ester oligomer chemosensor **CM10** with other reported chemosensors for  $\text{Fe}^{3+}$ .

### CONCLUSION

Curcumin-based ester oligomers with different lengths of alkyl side chains were successfully synthesized and characterized. The synthesized ester oligomers were soluble in most of the common organic solvents. Thermal stability of the synthesized oligomers was affected by the length of the alkyl side chains. The longer the alkyl side chains, the lower the ester oligomer thermal stability. The synthesized curcumin-based ester oligomers showed selectivity towards  $\text{Fe}^{3+}$  in which their fluorescence intensity decreased with increasing  $\text{Fe}^{3+}$  concentration. The detection limit of  $\text{Fe}^{3+}$  was 7.90  $\mu\text{M}$ .

### ACKNOWLEDGEMENT

The author would like to express gratitude to Universiti Sains Malaysia for the research facilities. This work was financially supported by 1001.PKIMIA.8011084 (USM Research University Research Grant) and 304.PKIMIA.6316060 (USM Bridging Research Grant).

### REFERENCES

- Nayak, S. K., Mohanty, S., Unnikrishnan, L. (2017) Trends and Applications in Advanced Polymeric Material, John Wiley & Sons, USA.
- Jain, V., Kokil, A. (2015) Optical Properties of Functional Polymers and Nano Engineering Applications, CRC Press Taylor & Francis Group, New York.
- Wang, J. W., Lv, F. T., Liu, L. B., Ma, Y. G., Wang, S. (2018) Strategies to Design Conjugated Polymer Based Materials for Biological Sensing and Imaging, *Coord. Chem. Rev.*, **354**, 135-154.
- Wu, W. B., Bazan, G. C., Liu, B. (2017) Conjugated-Polymer-Amplified Sensing, Imaging and Therapy, *Chem*, **2**, 760-790.
- Qu, Y., Wu, Y. Q., Gao, Y. T., Qu, S. Y., Yang, L., Hua, J. L. (2014) Diketopyrrolopyrrole-Based Fluorescent Conjugated Polymer for Application of Sensing Fluoride ion and Bioimaging, *Sensor Actuat. B-Chem.*, **197**, 13-19.
- Yang, P. C., Li, S. Q., Chien, Y. H., Tao, T. L., Huang, R. Y., Chen, H., Y. (2017) Synthesis, Chemosensory Properties, and Self-Assembly of Terpyridine-Containing Conjugated Polycarbazole through RAFT Polymerization and Heck Coupling Reaction, *Polymers*, **9**, 427.
- Chittigori, J., Kumar, A., Li, L., Thoa, S., Kokil, A., Sameulson, L., Sandman, D. J., Kumar, J. (2014) Synthesis of A Self Organizable Curcumin Derivative and Investigation of Its Interaction with Metals in 100% Aqueous Media, *Tetrahedron*, **70**, 991-995.
- Hu, L. J., Li, M., Zhang, Z. P., Shen, Y. Y., Guo, S. R. (2018) Self-assembly of Biotinylate Poly(ethylene glycol)-poly(curcumin) for Paclitaxel Delivery, *Int. J. Pharm.*, **553**, 510-521.
- Waghela, B. N., Sharma, A., Dhumale, S., Pandey, S. M., Pathak, C. (2015) Curcumin Conjugated with PLGA Potentiates Sustainability, Anti-Proliferative Activity and Apoptosis in Human Colon Carcinoma Cells, *PLoS One*, **10**, e0117526.
- Yang, R. L., Zhang, S., Kong, D. L., Gao, X. L., Zhao, Y. J., Wang, Z. S. (2012) Biodegradable Polymer-Curcumin Conjugate Micelles Enhance the Loading and Delivery of Low-Potency Curcumin, *Pharm. Res.*, **29**, 3512-3525.
- Nechifor, M. (2016) Aromatic Polyesters with Photosensitive Side Chains: Synthesis, Characterization and Properties, *J. Serb. Chem. Soc.*, **81**, 673-685.
- Schroeder, B. C., Nielsen, C. B., Westacott, P., Smith, J., Rossbauer, S., Anthopolos, T. D., Stingelin, N., McCulloch, I. (2015) Effects of Alkyl Chain Positioning on Conjugated Polymer Microstructure and Field-Effect Mobilities, *MRS Commun.*, **5**, 435-440.
- Kantheti, S., Narayan, R., Raju, K. V. S. N. (2015) The Impact of 1,2,3-Triazoles in The Design of Functional Coatings, *RSC. Adv.*, **5**, 3687-3708.
- Kim, J. S., Park, S. Y., Kim, S. H., Thuery, P., Souane, R., Matthews, S. E., Vicens, J. (2010) A Pyrenyl-Appended Triazole-Based Calix[4]arene as A Fluorescent Sensor for Iodide Ion, *Bull. Korean. Soc.*, **31**, 624-629.
- Zhao, Q., Wu, W. (2009) Syntheses and Photoluminescence Properties of UV Photocrosslinkable Polyesters based on fluorene, *Polym*, **50**, 998-1004.
- Kihara, M., Kohama, S. I., Umezono, S., Wakabayashi, K., Yamazaki, S., Kimura, K. (2011)

- Preparation of Poly(*p*-oxybenzoyl) Crystals Using Direct Polymerization of *p*-Hydroxybenzoic Acid in The Presence of Boronic Anhydrides, *J. Polym. Sci. Pol. Chem.*, **49**, 1088-1096.
17. Ravikumar, L., Prasad, M. B., Vasanthi, B. J., Gopalakrishnan, K., Rajeshkumar, J., Sengodan, V. (2009) Synthesis, Characterization and electrical conductivity of new poly(azomethineester)s from hydroxy acids, *Mater. Chem. Phys.* **115**, 632-636.
  18. Payton, F., Sandusky, P., Alworth, W. L. (2007) NMR Study of The Solution Structure of Curcumin, *J. Nat. Prod.*, **70**, 143-146.
  19. Lim, W. L., Oo, C. W. (2015) Intensity Enhancement of Photoluminescent Polyester by Photocrosslinking. *Polym. Int.*, **64**, 1433-1441.
  20. Zhang, X., Li, Z. C., Lao, C. F., Zou, D. C., Lu, F. Z., Chen, G. Q., Du, F. S., Li, F. M. (2006)  $\beta$ -diketone-Containing Styrenic Monomers and Their Polymers: Synthesis, Keto-enol Tautomerism and Related Fluorescence Behaviour, *Polymer*, **47**, 3390-3400.
  21. Qu, S. Z., Zheng, C. H., Liao, G. M., Fan, C. B., Liu, G., Pu, S. Z. (2017) A Fluorescent Chemosensor for  $\text{Sn}^{2+}$  and  $\text{Cu}^{2+}$  Based On a Carbazole-Containing Diarylethene, *RSC Adv.*, **7**, 9833.
  22. Ngororabanga, J. M., Plessis, J. D., Mama, N., (2017) Fluorescent Polymer Incorporating Triazolyl Coumarin Units for  $\text{Cu}^{2+}$  Detection via Planarization of Ict-Based Fluorophore, *Sensors*, **17**, 1980.
  23. Sharma, A., Enderlein, J., Kumbhakar. M. (2017) Photon Antibunching Reveals Static and Dynamic Quenching Interaction of Tryptophan with Atto-655, *J. Phys. Chem. Lett.*, **8**, 5821-5826.
  24. Bijian, R., Arun, K. B., Bappaditya, G., Partha, S. M. (2013) Fluorescent Tris-imidazolium Sensors for Picric Acid Explosive, *J. Org. Chem.*, **78**, 1306-1310.
  25. Geng, T. M., Wang, X., Zhu, F., Jiang, H., Wang, Y. (2017) Sensing of Polymeric Sensor-Based Rhodamine B Derivative for Metal Cations in Complete Aqueous Solution, *Bull. Mater. Sci.*, **40**, 187-193.
  26. Asaffar, M. S., Suhaimi, J. M., Ahmad Kabir, N. (2016) Evaluation of Heavy Metals in Surface Water of Major Rivers in Penang, *Int. J., Environ.*, **6**, 657-669.
  27. Y, D. L., Dai, C. H., Hu, Y. L., Liu, S. L., Weng, L. X., Luo, Z. M., Cheng, Y. X., Wang, L. H. (2017) A New Polymer-Based Fluorescent Chemosensor Incorporating Propane-1,3-dione and 2,5-diethynylbenzene Moieties for Detection of Copper (II) and Iron (III), *Polymers*, **9**, 267.
  28. Vanjare, B. D., Mahajan, P. G., Hong, S. K. (2018) Discriminating Chemosensor for Detection of  $\text{Fe}^{3+}$  in Aqueous Media by Fluorescence Quenching Methodology, *Bull. Korean Chem. Soc.*, **39**, 11442.
  29. Kim, Y. S., Lee, J. J., Lee, S. Y., Jo, T. G., Kim, C. (2016) A Highly Sensitive Benzimidazole-based Chemosensor for the Colorimetric detection of Fe (II) and Fe (III) and the fluorometric detection of Zn (II) in aqueous media, *RSC Adv.*, **6**, 61505-61515.
  30. Zhou, C., Zhang, Y., Liu, H. (2018) A Novel Nanofibrous Film Chemosensor for Detecting and Adsorbing  $\text{Fe}^{3+}$ , *J. Braz. Chem. Soc.*, **29**, 1678-4790.
  31. Hasan, S., Zakaria, S., Mohd Adnan, S. N. A. (2017) Fluorescent Chemosensor Bearing Amine and Benzenyl Functionality for  $\text{Fe}^{3+}$  Ions Detection in Aqueous Solution, *Int. J. Chem. Eng. Appl.*, **8**, 626.